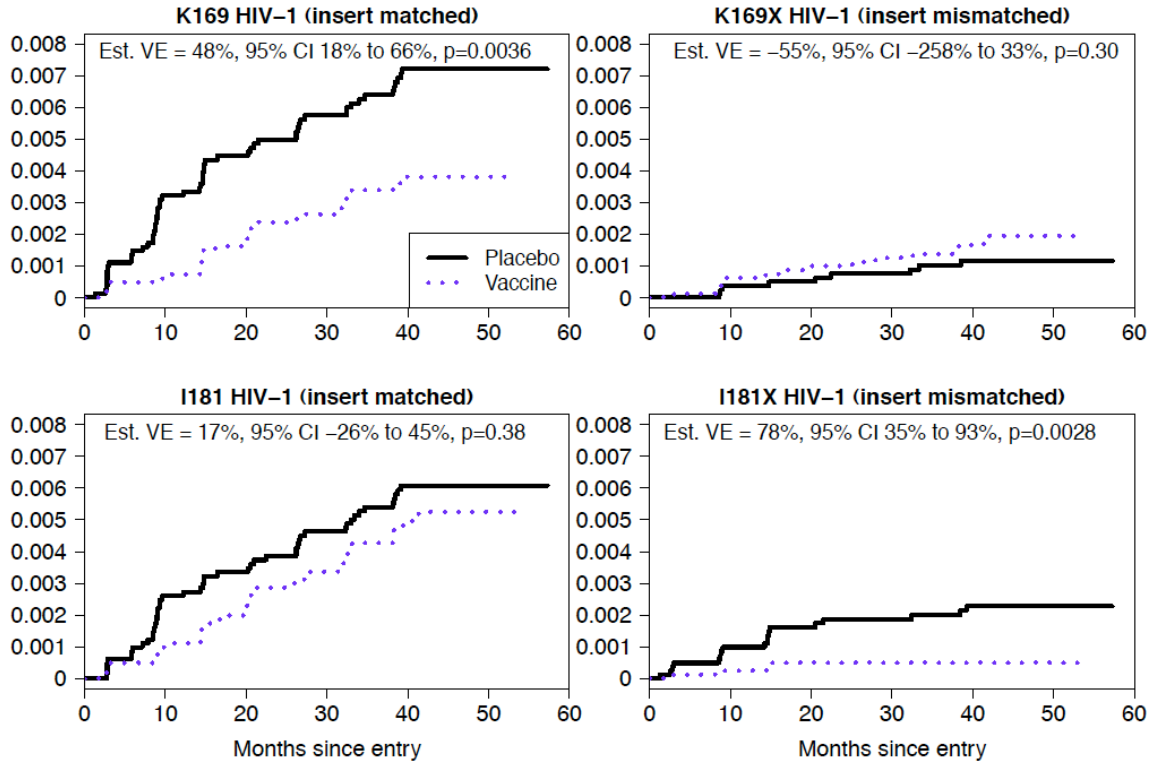
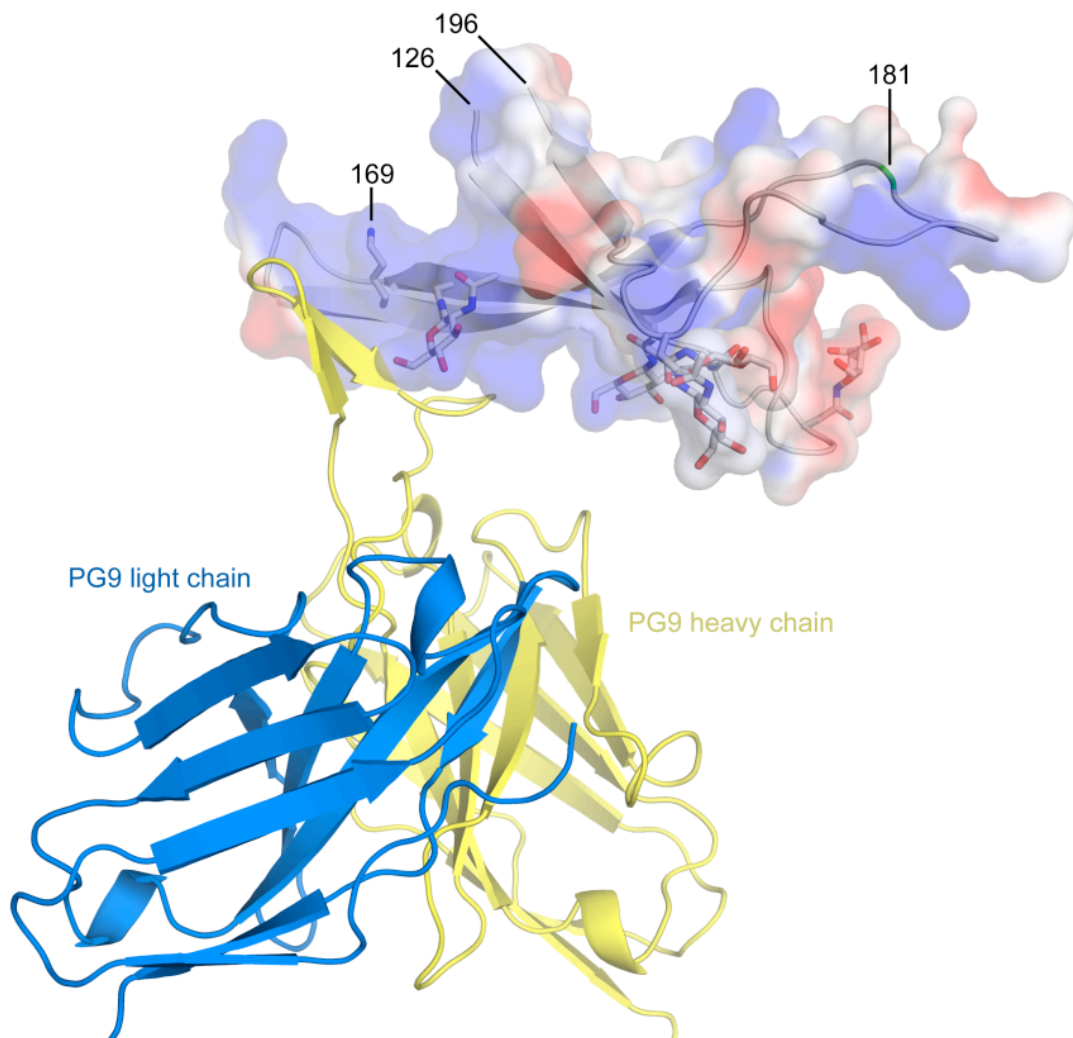


Supplementary Figure S1. Summary diagram.

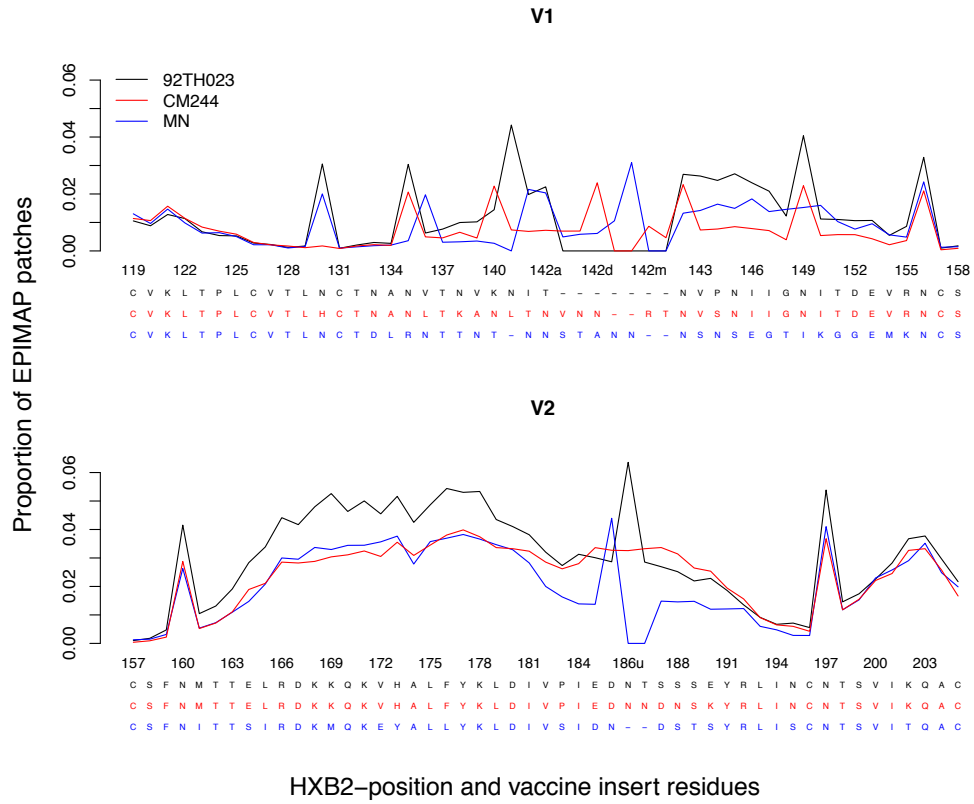


Supplementary Figure S2. Estimated cumulative probabilities of genotype-specific HIV infection. The cumulative probabilities were estimated by the method of Kaplan-Meier based on all RV144 participants: 8,197 vaccine and 8,198 placebo recipients. For each of the genotypes, the curves for the vaccine and placebo groups did not cross, showing that the most misleading kind of violation of the proportional hazards assumption did not occur. The Grambsch and Therneau proportional hazards test (based on Schoenfeld residuals) (ref. 30) did not reject the proportional hazards assumption for any of the genotypes ((K169: p=0.12; K169X: p=0.90; I181: p=0.14; I181X: p=0.38). The trend for K169 and I181 (p=0.12, 0.14) could be potentially concerning; however, we note that the vaccine efficacy derived from the proportional hazards model still has a meaningful interpretation if the proportional hazards assumption does not perfectly hold (barring crossing hazards), namely as a time-averaged vaccine efficacy which conveys information on the average reduction in the hazard rate (vaccine versus placebo) over time. The genotype-specific analysis suggested that vaccine-efficacy waned over time. This is in agreement with the main RV144 results where vaccine efficacy was estimated at 60% in the first year of the trial, before declining rapidly afterwards (ref.12).

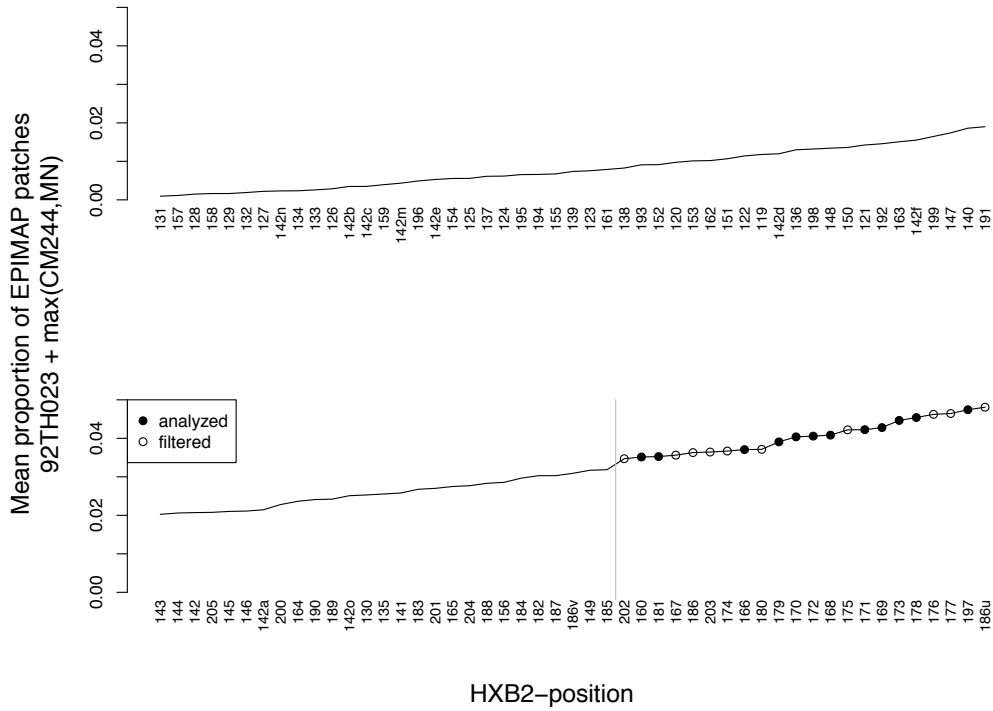


Supplementary Figure S3. V1/V2 bound to antibody PG9.

The signature sites 169 and 181 are identified in a model of the complete V1/V2 region bound by PG9 (ref. 23). The C α -C α distance between these sites is approximately 37 Å. The variable domains of PG9 are shown as yellow (heavy chain) and blue (light chain) ribbons. The V1/V2 region is shown as grey ribbons with a semi-transparent molecular surface colored by electrostatic potentials, positive (blue) to negative (red), +1 to -1 kT/e, respectively. N-acetylglucosamine moieties are shown as sticks attached to asparagine residues.



Supplementary Figure S4. Proportion of EPIMAP patches including a given V1/V2 site. Statistics were calculated against the three vaccine inserts.



Supplementary Figure S5. V1/V2 sites ranked based on the mean proportion of EPIMAP patches calculated against the three vaccine inserts.

The highest ranking V1/V2 sites were identified based on the average of the proportion for the prime (92TH023) and the maximum of the two boost proteins (MN,CM244); the top 22 sites were selected for further analysis.

Supplementary Methods S1. Env-V1/V2 sites selected for analysis.

In addition to the HXB2 reference sequence, the vaccine insert sequences (prime: 92TH023; boost: MN and CM244) are figured with the consensus and second AA found in the sequenced vaccine and placebo breakthrough viruses (based on the consensus sequences for each of the 110 subjects infected with CRF01_AE).

Sites that passed the conservation criteria are in grey. Sites that were excluded because they were too conserved are represented with 'C', sites excluded because they were too variable to be aligned with confidence are represented with 'V'.

The sites selected in the first screening approach (Approach 1 'Contact residues') correspond to those that passed the conservation criteria, were detected as hotspots in a peptide microarray analysis ('Ab array') and identified as either antibody contact sites ('Ab contact') or through previous studies ('Literature') ('T': Tomaras et al., 2011(ref. 10); 'M': Moore et al., 2009 (ref. 9); 'W': Wei et al., 2003 (ref. 8)).

The sites selected in the second screening approach (Approach 2 'EPIMAP') correspond to those that passed the conservation criteria and were predicted as hotspots through the EPIMAP approach.

We had pre-specified multiple filters (such as conservation levels, prior evidence in the literature) and particular combinations of these filters to employ for analysis, we resolved (before performing any analysis) to first apply the most conservative filtering option, which is the intersection of the specified filters.

The 'Contact residues' and 'EPIMAP' filters did not select the same sites for downstream analyses, which were performed independently (i.e., the two sets of sites derived from approaches #1 and #2 are not combined).

The alternative approach with the 'EPIMAP' filter identified potential contact sites through purely structural-prediction means. We selected the top 20 predicted sites in the 85-site gp70-V1/V2 region (because of a drop-off in the prediction scores after the first 20), of which 12 passed the "invariant sites" and "alignability" filters.

Note that there are three distinct inserts used in the RV144 vaccine that overlap the 85-AA V1/V2 region, and the analyses were separately conducted for each insert, as pre-specified. The invariant sites filter depends on the analysis method only through the number of sequences per subject used for the method (the Model-based and GWJ methods use one sequence per subject, and the MMBootstrap method uses all available sequences per subject).

Supplementary Table S1. Differential vaccine efficacy (VE) against three vaccine insert sequences (92TH023 (prime), CM244 and MN) using sites pre-selected via the ‘contact residues’ and ‘EPIMAP’ approaches. Results were calculated using the Cox proportional hazards model as adapted by Lunn and McNeil (ref. 28) and Gilbert (ref. 29) based on both the dataset of sequences from 110 and 109 subjects (one subject from a linked pair was excluded). Significant p- and q-values are in bold.

Contact residues - 110 subjects						
	92Th023		CM244		MN	
HXB2 Pos.	p-value	q-value	p-value	q-value	p-value	q-value
120	0.183	0.488	0.183	0.488	0.183	0.549
124	0.881	0.881	0.881	0.881	0.881	0.881
165	0.685	0.783	0.685	0.783	0.794	0.881
166	0.472	0.755	0.472	0.755	NA	NA
168	0.620	0.783	0.620	0.783	0.620	0.881
169	0.025	0.104	0.025	0.104	NA	NA
171	0.314	0.627	0.314	0.627	0.314	0.627
181	0.026	0.104	0.026	0.104	0.026	0.155

Contact residues - 109 subjects						
	92Th023		CM244		MN	
HXB2 Pos.	p-value	q-value	p-value	q-value	p-value	q-value
120	0.352	0.705	0.352	0.705	0.352	0.705
124	0.907	0.907	0.907	0.907	0.907	0.907
165	0.619	0.741	0.619	0.741	0.736	0.883
166	0.529	0.741	0.529	0.741	NA	NA
168	0.648	0.741	0.648	0.741	0.648	0.883
169	0.039	0.157	0.039	0.157	NA	NA
171	0.275	0.705	0.275	0.705	0.275	0.705
181	0.029	0.157	0.029	0.157	0.029	0.174

EPIMAP - 110 subjects						
	92Th023		CM244		MN	
HXB2 Pos	p-value	q-value	p-value	q-value	p-value	q-value
160	0.794	0.999	0.794	0.999	0.794	0.999
166	0.472	0.944	0.472	0.944	NA	NA
168	0.620	0.962	0.620	0.962	0.620	0.999
169	0.025	0.155	0.025	0.155	NA	NA
170	0.929	0.999	0.929	0.999	0.929	0.999
171	0.314	0.836	0.314	0.836	0.314	0.705
172	0.641	0.962	0.641	0.962	NA	NA
173	0.348	0.836	0.348	0.836	0.101	0.454
178	0.275	0.836	0.275	0.836	0.275	0.705
179	0.872	0.999	0.872	0.999	0.872	0.999
181	0.026	0.155	0.026	0.155	0.026	0.233
197	0.999	0.999	0.999	0.999	0.999	0.999

EPIMAP - 109 subjects						
	92Th023		CM244		MN	
HXB2 Pos.	p-value	q-value	p-value	q-value	p-value	q-value
160	0.824	0.925	0.824	0.925	0.824	0.954
166	0.529	0.925	0.529	0.925	NA	NA

168	0.648	0.925	0.648	0.925	0.648	0.954
169	0.039	0.235	0.039	0.235	NA	NA
170	0.767	0.925	0.767	0.925	0.767	0.954
171	0.275	0.705	0.275	0.705	0.275	0.619
172	0.687	0.925	0.687	0.925	NA	NA
173	0.294	0.705	0.294	0.705	0.122	0.548
178	0.200	0.705	0.200	0.705	0.200	0.600
179	0.848	0.925	0.848	0.925	0.848	0.954
181	0.029	0.235	0.029	0.235	0.029	0.262
197	0.980	0.980	0.980	0.980	0.980	0.980

Supplementary Table S2. Genotype-specific analysis of correlates of risk variables.

We repeated the statistical method used in Haynes and colleagues (ref. 2) to assess correlates of risk of HIV-1 infection with the gp70-V1/V2 antibody binding and the V2 hotspot variables on the subset of HIV-1 infections that were genetically characterized. There were 41 vaccine recipient cases in the case-control study, where a case means HIV-1 negative at week-24 and infected afterwards. Of the 41 vaccine recipient cases, we could only include those infected with HIV-1 CRF01_AE, i.e. 34 subjects. 25 infections corresponded to K169 variants and 9 were K169X, while 31 infections corresponded to I181 variants and 3 were I181X. For each of the 4 genotypes (K169, K169X, I181, I181X), we applied the statistical method used in Haynes and colleagues (ref. 2) to assess the gp70-V1/V2 antibody binding and the V2 hotspot variables, which were respectively a primary and secondary variable in Haynes and colleagues. Gp70-V1/V2 was assessed as a quantitative variable, and the relative risk (RR) of infection was estimated per standard deviation change in antibody level among vaccine recipients; in contrast, the V2 hotspot variable was assessed as dichotomous: the relative risk of infection was estimated for vaccine recipients with or without positive reactivity to the V2 hotspot.

HIV genotype	Number of infections	Estimated RR (95% C.I.)	p-value
gp70-V1/V2 Abs			
K169	25	0.65 (0.40,1.03)	0.068
K169X	9	0.69 (0.33,1.46)	0.34
I181	31	0.56 (0.36,0.87)	0.01
I181X	3	2.03 (0.61,6.7)	0.25
V2 hotspot Abs			
K169	25	0.64 (0.39,1.05)	0.079
K169X	9	0.71 (0.31,1.61)	0.41
I181	31	0.57 (0.36,0.92)	0.021
I181X	3	1.6 (0.50,5.14)	0.43

Regarding site 169, the results show that the correlates of risk are slightly stronger for K169-matched infections compared to K169X-mismatched infections, which is consistent with the hypothesis of V2-directed antibodies as a possible correlate of protection. However, the dataset is too small (especially when broken down to specific HIV-1 genotypes) to provide adequate statistical power to demonstrate a stronger correlate of risk against K169-infections, and there is no statistical evidence that this occurred.

Regarding site 181, the results for I181X-mismatched infections have very low power and precision, given that they correspond to only 3 infected vaccine recipients. Therefore, only the results for I181-matched infections are precise enough to interpret: both antibody variables were significant inverse correlates of infection rate, a result that is consistent with the positive vaccine efficacy against I181-viruses (estimated at 17%) reported in the main text. Since the interactions between the antibody variables and the genotypes are not significant, these results do not statistically support an interpretation that the sieve effects are explained by the previously reported correlate of risk.

Supplementary Table S3. Identification of signature sites by three site-scanning methods (GWJ, MMBootstrap, Model-based) against three vaccine insert sequences (92TH023 (prime), MN and CM244) using sites pre-selected via the 'contact residues' and 'EPIMAP' approaches. Results are presented based on both the dataset of sequences from 110 or 109 subjects (one subject from a linked pair excluded). Significant p- and q-values are in bold. A summary of the methods used is found below the table.

Contact residues - 110 subjects						
92Th023	GWJ		MMBootstrap		Model-based	
HXB2 Pos.	p-value	q-value	p-value	q-value	p-value	q-value
120	0.398	0.707	0.102	0.273	0.334	0.534
124	1.000	1.000	0.868	0.918	0.786	0.786
165	0.684	0.889	0.802	0.918	0.740	0.786
166	0.442	0.707	0.428	0.685	0.276	0.534
168	0.778	0.889	0.918	0.918	0.654	0.786
169	0.018	0.077	0.042	0.168	<i>0.050</i>	<i>0.202</i>
171	0.322	0.707	0.298	0.596	0.250	0.534
181	0.019	0.077	0.035	0.168	0.021	0.165
CM244	GWJ		MMBootstrap		Model-based	
HXB2 Pos.	p-value	q-value	p-value	q-value	p-value	q-value
120	0.398	0.707	0.102	0.273	0.334	0.534
124	1.000	1.000	0.868	0.918	0.786	0.786
165	0.684	0.889	0.802	0.918	0.740	0.786
166	0.442	0.707	0.428	0.685	0.276	0.534
168	0.778	0.889	0.918	0.918	0.654	0.786
169	0.018	0.077	0.042	0.168	<i>0.050</i>	<i>0.202</i>
171	0.322	0.707	0.298	0.596	0.250	0.534
181	0.019	0.077	0.035	0.168	0.021	0.165
MN	GWJ		MMBootstrap		Model-based	
HXB2 Pos.	p-value	q-value	p-value	q-value	p-value	q-value
120	0.398	0.796	0.102	0.307	0.334	0.668
124	1.000	1.000	0.868	0.918	0.786	0.786
165	0.702	0.934	0.816	0.918	0.662	0.786
168	0.778	0.934	0.918	0.918	0.586	0.786
171	0.322	0.796	0.298	0.596	0.270	0.668
181	0.019	0.116	<i>0.035</i>	<i>0.209</i>	0.022	0.134

Contact residues - 109 subjects						
92Th023	GWJ		MMBootstrap		Model-based	
HXB2 Pos.	p-value	q-value	p-value	q-value	p-value	q-value
124	1.000	1.000	0.860	0.918	0.824	0.824

165	0.658	0.896	0.660	0.918	0.652	0.824
166	0.506	0.886	0.558	0.918	0.332	0.581
168	0.768	0.896	0.918	0.918	0.718	0.824
169	0.030	0.105	0.078	0.274	0.061	0.214
171	0.262	0.611	0.250	0.583	0.232	0.541
181	0.023	0.105	<i>0.044</i>	<i>0.274</i>	0.025	0.178

CM244	GWJ		MMBootstrap		Model-based	
HXB2 Pos.	p-value	q-value	p-value	q-value	p-value	q-value
124	1.000	1.000	0.860	0.918	0.824	0.824
165	0.658	0.896	0.660	0.918	0.652	0.824
166	0.506	0.886	0.558	0.918	0.332	0.581
168	0.768	0.896	0.918	0.918	0.718	0.824
169	0.030	0.105	0.078	0.274	0.061	0.214
171	0.262	0.611	0.250	0.583	0.232	0.541
181	0.023	0.105	<i>0.044</i>	<i>0.274</i>	0.025	0.178

MN	GWJ		MMBootstrap		Model-based	
HXB2 Pos.	p-value	q-value	p-value	q-value	p-value	q-value
124	1.000	1.000	0.860	0.918	0.824	0.824
165	0.656	0.960	0.694	0.918	0.654	0.818
168	0.768	0.960	0.918	0.918	0.630	0.818
171	0.262	0.655	0.250	0.625	0.244	0.610
181	0.023	0.114	<i>0.044</i>	<i>0.218</i>	0.026	0.128

EPIMAP - 110 subjects

92Th023	GWJ		MMBootstrap		Model-based	
HXB2 Pos	p-value	q-value	p-value	q-value	p-value	q-value
160	0.670	0.904	0.850	0.918	0.860	0.946
166	0.442	0.810	0.428	0.814	0.260	0.590
168	0.778	0.904	0.918	0.918	0.780	0.946
169	0.018	0.106	<i>0.042</i>	<i>0.232</i>	<i>0.049</i>	<i>0.272</i>
170	0.822	0.904	0.812	0.918	0.860	0.946
171	0.322	0.708	0.298	0.814	0.268	0.590
172	0.620	0.904	0.544	0.855	0.560	0.946
173	0.304	0.708	0.444	0.814	0.860	0.946
178	0.194	0.708	0.426	0.814	0.126	0.461
179	0.912	0.912	0.686	0.918	1.000	1.000
181	0.019	0.106	<i>0.035</i>	<i>0.232</i>	<i>0.026</i>	<i>0.272</i>

CM244	GWJ		MMBootstrap		Model-based	
HXB2 Pos	p-value	q-value	p-value	q-value	p-value	q-value

160	0.670	0.904	0.850	0.918	0.860	0.946
166	0.442	0.810	0.428	0.814	0.260	0.590
168	0.778	0.904	0.918	0.918	0.780	0.946
169	0.018	0.106	0.042	0.232	0.049	0.272
170	0.822	0.904	0.812	0.918	0.860	0.946
171	0.322	0.708	0.298	0.814	0.268	0.590
172	0.620	0.904	0.544	0.855	0.560	0.946
173	0.304	0.708	0.444	0.814	0.860	0.946
178	0.194	0.708	0.426	0.814	0.126	0.461
179	0.912	0.912	0.686	0.918	1.000	1.000
181	0.019	0.106	0.035	0.232	0.026	0.272

MN	GWJ		MMBootstrap		Model-based	
HXB2 Pos	p-value	q-value	p-value	q-value	p-value	q-value
160	0.670	0.912	0.850	0.918	0.860	0.983
168	0.778	0.912	0.918	0.918	0.420	0.672
170	0.822	0.912	0.812	0.918	0.840	0.983
171	0.322	0.644	0.298	0.795	0.280	0.560
173	0.087	0.347	0.058	0.230	0.171	0.457
178	0.194	0.517	0.426	0.852	0.128	0.457
179	0.912	0.912	0.686	0.918	1.000	1.000
181	0.019	0.155	0.035	0.230	0.026	0.210

EPIMAP - 109 subjects

92Th023	GWJ		MMBootstrap		Model-based	
HXB2 Pos.	p-value	q-value	p-value	q-value	p-value	q-value
160	0.690	0.845	0.900	0.982	0.844	0.928
166	0.506	0.845	0.558	0.836	0.340	0.748
168	0.768	0.845	0.918	0.982	0.630	0.866
169	0.030	0.165	0.078	0.431	0.061	0.333
170	0.676	0.845	0.982	0.982	0.602	0.866
171	0.262	0.612	0.250	0.688	0.232	0.638
172	0.692	0.845	0.558	0.836	0.448	0.821
173	0.278	0.612	0.362	0.796	0.822	0.928
178	0.160	0.587	0.222	0.688	0.103	0.376
179	0.890	0.890	0.608	0.836	0.948	0.948
181	0.023	0.165	0.044	0.431	0.026	0.288

CM244	GWJ		MMBootstrap		Model-based	
HXB2 Pos.	p-value	q-value	p-value	q-value	p-value	q-value
160	0.690	0.845	0.900	0.982	0.844	0.928
166	0.506	0.845	0.558	0.836	0.340	0.748
168	0.768	0.845	0.918	0.982	0.630	0.866

169	0.030	0.165	0.078	0.431	0.061	0.333
170	0.676	0.845	0.982	0.982	0.602	0.866
171	0.262	0.612	0.250	0.688	0.232	0.638
172	0.692	0.845	0.558	0.836	0.448	0.821
173	0.278	0.612	0.362	0.796	0.822	0.928
178	0.160	0.587	0.222	0.688	0.103	0.376
179	0.890	0.890	0.608	0.836	0.948	0.948
181	0.023	0.165	<i>0.044</i>	<i>0.431</i>	<i>0.026</i>	<i>0.288</i>

MN	GWJ		MMBootstrap		Model-based	
	p-value	q-value	p-value	q-value	p-value	q-value
HXB2 Pos.						
160	0.690	0.878	0.900	0.982	0.844	0.965
168	0.768	0.878	0.918	0.982	0.692	0.923
170	0.676	0.878	0.982	0.982	0.628	0.923
171	0.262	0.524	0.250	0.500	0.244	0.488
173	0.115	0.427	0.080	0.320	0.184	0.488
178	0.160	0.427	0.222	0.500	0.100	0.400
179	0.890	0.890	0.608	0.973	1.000	1.000
181	0.023	0.183	<i>0.044</i>	<i>0.320</i>	<i>0.026</i>	<i>0.204</i>

Site-scanning sieve analysis methods evaluate each site to identify those that discriminate the vaccine and placebo group. In addition to the differential VE analysis, the pre-selected sites were tested against the three vaccine insert sequences using three other methods: a nonparametric weighted distance comparison test (GWJ) (ref. 13), a Mismatch Bootstrap method (MMBootstrap) adapted from (ref. 7), and a model-based Bayesian-frequentist hybrid method that is more sensitive to differences in non-insert AA frequencies (ref.14: <http://arxiv.org/abs/1206.6701>). The GWJ method computes a two-sample pooled-variance t-statistic and compares this statistic to a permutation-derived null distribution. Each subject contributes a weight that is computed as the from-insert-AA-to-subject-AA entry in a (probability-form) substitution matrix (the 1% diverged between-subject HIV-1 matrix (Nickle, Heath, et al., PLoSOne, 2007), using the subject’s ‘mindist’ sequence. The MMBootstrap method computes the difference in the fraction of mismatches-to-the-insert-AA using all available sequences, and compares this to a bootstrap-derived null distribution (resampling subject labels, not individual sequence labels). The Model-based method compares the probability of the vaccine-recipient sequences given a “null” multinomial model with parameters estimated as being proportional to the observed placebo-recipient frequencies plus pseudocounts of 1/21 per category (20 AA and a gap-character category) to the “alternative” model probability that is computed as the expected value (over an “insert-only” indicator parameter, $i \sim \text{Bernoulli}(0.5)$), and a “sieve effect strength” parameter, $s \sim \text{Uniform}(0,1)$) of the probability of the vaccine-recipient sequences given a multinomial model in which the probability of the insert amino acid is multiplied by $(1-s)$ and the removed mass is reallocated either proportionally (if i is 1) or uniformly (if i is 0) among the remaining categories. All of these methods were verified for control of type-I error rate. A q-value multiplicity adjustment procedure was pre-specified to limit the false discovery rate to 20% (ref. 31); it was conducted on a per-analysis basis, i.e. per insert and per method.

Supplementary Table S4. Degree of correlated evolution between viral traits and treatment assignment measured with phylogenetically independent contrasts: Summary statistics for regression of contrasts through the origin.

	gp70	gp70	gp120	gp120	NFLG ^a	NFLG
Number of sequences	110	109	110	109	110	109
Absolute contrasts vs standard deviation						
p-value 'Vaccine'	0.079	0.109	0.347	0.902	0.515	0.606
p-value 'K169X'	0.817	0.766	0.902	0.472	0.224	0.240
p-value 'I181X'	0.943	0.561	0.644	0.207	0.240	0.106
Number of contrasts	109	108	109	108	109	108
Contrasts: X = 'Vaccine'; Y = 'K169X'						
Pearson Rho	0.053	0.061	0.032	0.042	0.056	0.054
Least Squares Regression:						
r ²	0.003	0.004	0.001	0.002	0.003	0.003
2-tailed p-value	0.580	0.530	0.739	0.668	0.559	0.575
Number of Y contrasts > 0	36	39	33	33	36	40
Number of Y contrasts < 0	29	29	30	29	45	41
Number of Y contrasts = 0	44	40	46	46	28	27
Contrasts: X = 'Vaccine'; Y = 'I181X'						
Pearson Rho	-0.246	-0.248	-0.267	-0.319	-0.257	-0.254
Least Squares Regression:						
r ²	0.061	0.061	0.072	0.102	0.066	0.065
2-tailed p-value	0.010	0.009	0.005	0.001	0.007	0.008
Number of Y contrasts > 0	23	22	27	29	33	37
Number of Y contrasts < 0	38	36	37	38	48	44
Number of Y contrasts = 0	48	50	45	41	28	27
Contrasts: X = 'K169X'; Y = 'I181X'						
Pearson Rho	-0.026	-0.036	0.032	0.051	0.080	0.088
Least Squares Regression:						
r ²	0.001	0.001	0.001	0.003	0.006	0.008
2-tailed p-value	0.791	0.709	0.741	0.596	0.408	0.795
Number of Y contrasts > 0	35	28	41	36	25	31
Number of Y contrasts < 0	26	30	23	31	25	28
Number of Y contrasts = 0	48	50	45	41	59	49

^aNFLG: near full-length genome sequences (alignment length: 8,577 nucleotides).

^bPhylogenetically independent contrasts between the vaccine status and the tip data were calculated using the PDAP:PDTREE implementation of Garland and colleagues (Garland, Am. Nat., 1992) in Mesquite (http://mesquiteproject.org/pdap_mesquite/).

Supplementary Table S5. Phylogenetic dependency network based on an *env* tree.
 Only the results for the sites that passed our filtering criteria are given; the method is described in ref.16.

Filter	HXB2 position	p-value	q-value	Predictor	Target AA	Consensus
Contact residues	120	>0.05				
Contact residues	124	>0.05				
EPIMAP	160	>0.05				
Both	165	>0.05				
Both	166	>0.05				
Both	168	>0.05				
Both	169	>0.05				
EPIMAP	170	>0.05				
Both	171	>0.05				
EPIMAP	172	>0.05				
EPIMAP	173	0.0321	0.8546	vaccine	Y	Y
EPIMAP	178	>0.05				
EPIMAP	179	>0.05				
Both	181	0.0245	1	vaccine	M	I
EPIMAP	197	>0.05				

The filter refers to the approach used to select sites for statistical tests, either the 'contact residues' or 'EPIMAP' approach; 'both' refers to sites that were selected by both the contact residues and EPIMAP approaches.

Supplementary Table S6. Differential selective pressure between vaccine and placebo groups. Likelihood ratio test to identify sites that are evolving in the two populations under different selective pressures along internal tree branches, as implemented in Hyphy (ref. 18) (<http://www.hyphy.org>).

Filter	HXB2 position	LRT (110)^a	p-value (110)	LRT (109)	p-value (109)
Contact residues	120	0.005	0.941	0.005	0.945
Contact residues	124	0	0.996	0.252	0.615
EPIMAP	160	2.671	0.102	4.37	0.037
Both	165	1.811	0.178	2.372	0.124
Both	166	0.924	0.337	0.525	0.469
Both	168	0.058	0.81	0.104	0.747
Both	169	4.105	0.043	3.422	0.064
EPIMAP	170	0	0.985	0.042	0.838
Both	171	0	0.998	0	0.996
EPIMAP	172	2.002	0.157	1.374	0.241
EPIMAP	173	2.967	0.085	3.833	0.05
EPIMAP	178	0.154	0.694	0.216	0.642
EPIMAP	179	2.527	0.112	1.958	0.162
Both	181	0.054	0.817	0.022	0.881
EPIMAP	197	2.778	0.096	2.257	0.133

The filter refers to the approach used to select sites for statistical tests, either the 'contact residues' or 'EPIMAP' approach; 'both' refers to sites that were selected by both the contact residues and EPIMAP approaches.

^aThe number in parenthesis corresponds to the number of subjects in the analysis. The set of 110 includes all the individuals infected with HIV-1 CRF01_AE; Sequences from one of the two individuals in the linked transmission pair was removed from the set of 109.

Supplementary Table S7. Comparison of the length of the V2 loop and number of PNGS and relationship with the time of HIV-1 infection.

	K169	K169X	p-value
Mean V2 Loop length (IQR)	41.9 (39-44)	43.2 (40-46)	0.11
Mean V2 PNGS (IQR)	2.12 (2-3)	2.44 (2-3)	0.08
Mean Duration of infection (IQR)	207 (167-191)	250 (169-203)	0.41

Based on all the Env sequences from the 110 subjects, we calculated the V2 loop length and number of PNGS for each sequence and computed an average for each subject. The distribution of values between subjects carrying K169- or K169X-variants was compared using Mann-Whitney-Wilcoxon's tests.

The time of infection was estimated as the time since the last negative visit, as conventionally done in the context of vaccine trials. Given that visits were scheduled every six months in the trial, we note that this estimate of duration of HIV-1 infection is imprecise. Comparisons were done with Mann-Whitney-Wilcoxon's tests.

Supplementary Table S8. Distances between the C α atoms of the residues 169 and 181.

Distances were computed within the low energy models for the ALVAC-HIV and AIDSVAX B/E gp120 vaccine inserts.

Insert	Min.	Q1	Median	Mean	Q3	Max.	St Dev.
ALVAC_92TH023	7.68	17.04	21.81	22.71	28.45	35.98	7.04
AIDSVAX_MN	8.32	15.39	18.72	19.15	22.93	37.68	5.80
AIDSVAX_CM244	6.28	13.98	19.07	18.99	23.3	34.69	6.08
All inserts ^a	6.28	15.75	20.07	20.88	25.58	37.68	6.76

^aPredictions based on all three inserts combined.

Supplementary Table S9. Co-variation in the two sets of sites defined by the 'Contact residues' and 'EPIMAP' approaches.

Results are based on 2 methods: Kullback-Leibler (ref. 25) and Spidermonkey (which is phylogenetically-corrected) (ref. 26). Sites in bold are statistically significant and have q-values below the pre-specified threshold of 0.20.

Kullback-Leibler co-variation test:			
Vaccine group			
Site 1	Site 2	p-value	q-value
Contact residues (9 sites)			
120	122	0.0056	0.1008
165	166	0.0032	0.1008
165	168	0.0346	0.311
165	169	ns (.9251)	ns (1.0)
166	169	ns (.5275)	ns (1.0)
166	171	0.0432	0.311
169	171	0.0172	0.2064
EPIMAP (12 sites)			
168	173	0.0084	0.554
169	171	0.0184	0.607
170	178	0.0292	0.642
166	171	0.0398	0.657
Kullback-Leibler co-variation test:			
Placebo group			
Site 1	Site 2	p-value	q-value
Contact residues (9 sites)			
165	166	ns (.3616)	ns (1.0)
165	171	ns (.6553)	ns (1.0)
166	181	ns (.9251)	ns (1.0)
EPIMAP (12 sites)			
170	173	0.009	0.515
179	181	0.0156	0.515
Kullback-Leibler differential co-variation test:			
Vaccine vs placebo			
Site 1	Site 2	p-value	q-value
Contact residues (9 sites)			
120	171	ns (.0682)	ns (.2273)
122	171	0.0478	0.2273
165	169	0.0424	0.2273
166	169	0.0426	0.2273
169	171	ns (.0546)	ns (.2273)
EPIMAP (12 sites)			
168	178	0.005	0.33
169	170	0.0152	0.502
178	181	0.0334	0.601
166	169	0.0434	0.601

179	181	0.0468	0.601
169	171	0.0546	ns (.601)

Spidermonkey: Vaccine

Site 1	Site 2	$P(S1 \rightarrow S2)^a$	$P(S1 \leftarrow S2)^b$	$P(S1 \leftrightarrow S2)^c$
Contact residues (9 sites) (dataset with 44 subjects)				
165	168	0.297709	0.245925	0.543634
169	165	0.284427	0.248955	0.533382

Contact residues (9 sites) (dataset with 43 subjects)

No co-evolving selected sites

EPIMAP (12 sites) (dataset with 44 subjects)

160	169	0.26152	0.546533	0.808053
-----	-----	---------	----------	----------

EPIMAP (12 sites) (dataset with 43 subjects)

160	169	0.198658	0.676808	0.875466
171	181	0.433441	0.102533	0.535974

Spidermonkey: Placebo

Site 1	Site 2	$P(S1 \rightarrow S2)^a$	$P(S1 \leftarrow S2)^b$	$P(S1 \leftrightarrow S2)^c$
Contact residues (9 sites)				
166	165	0.198155	0.462487	0.660642
171	166	0.468572	0.26846	0.737032
181	165	0.188977	0.353574	0.542551

EPIMAP (12 sites)

172	166	0.181986	0.319073	0.501059
181	179	0.492802	0.242276	0.735078
197	168	0.074233	0.431484	0.505717

^aThe posterior probability for site 2 is conditionally dependent on site 1.

^bThe posterior probability for site 1 is conditionally dependent on site 2.

^cThe posterior probability for sites 1 and 2 are conditionally dependent.

Supplementary Table S10. CRF01_AE-specific PCR primers.

**Near-Full-length
Genome (NFLG)
PCR Primers**

1st Round Primers	Sequence	HXB2 start	HXB2 end	Direction	Usage
1.U5_deg	TGAGTGCTTMAAGTRGTGTGTGCCCGTCTGT	541	571	Forward	Main
1.3'3'pl_deg	CACYACTTKAAGCACTCAAGGCAAGCTTTATTG	9611	9643	Reverse	Main
2nd Round Primers					
2.U5-AE	AGTGGTGTGTGCCCGTCTGTGTTAGGACTC	552	581	Forward	Main
2.3'3'pl_deg	TKAAGCACTCAAGGCAAGCTTTATTGAGGCTT	9605	9636	Reverse	Main
Msf12b	AAATCTCTAGCAGTGGCGCCCGAACAG	653	634	Forward	Alternate
AE1R	GCAGCTGCTTATATGCAGGATCTGAGGG	9497	9524	Reverse	Alternate

5' Half Genome PCR Primers

1st Round Primers	Sequence	HXB2 start	HXB2 end	Direction
1.U5_deg	TGAGTGCTTMAAGTRGTGTGTGCCCGTCTGT	541	571	Forward
1.5'3'pl-deg	YTCCGCTTCTCCTGCCATAGGAGAT	5963	5988	Reverse
2nd Round Primers				
2.U5-AE	AGTGGTGTGTGCCCGTCTGTGTTAGGACTC	552	581	Forward
AE12R	TTCCCGGRTGKTTCCAGGGCTCTA	5853	5876	Reverse

3' Half Genome PCR Primers

1st Round Primers	Sequence	HXB2 start	HXB2 end	Direction
1.3'5'pl-AE	GGACAGTACATCTATAACAMTTATGGGGATACTT	5685	5718	Forward
1.3'3'pl_deg	CACYACTTKAAGCACTCAAGGCAAGCTTTATTG	9611	9643	Reverse
2nd Round Primers				
2.3'5'salpl	GGGTTGGGTGTCGACATAGCAGAATAGG	5777	5804	Forward
2.3'3'pl_deg	TKAAGCACTCAAGGCAAGCTTTATTGAGGCTT	9605	9636	Reverse

Supplementary Table S11. CRF01_AE-specific sequencing primers.

Primer Name	Sequence	HXB2 start	HXB2 end	Direction
AE1F	TGACTAGCGGAGGCTAGAAGGAGAGA	763	788	Forward
AE2F	GACACCAAGGAAGCTTTAGA	1075	1094	Forward
AE3F	ATGAGGAAGCTGCAGAATGGG	1406	1426	Forward
AE4F	ACAGGAGCAGATGATACAGTA	2328	2348	Forward
AE5F	CCAGGAATGGATGGACCAA	2589	2607	Forward
AE6F	CAATACATGGATGACTTGTATGTAGG	3093	3118	Forward
AE7F	CCATTTAAAAATCTAAAAACAGG	3582	3604	Forward
AE8F	ACTTTCTATGTAGATGGGGCAGC	3864	3886	Forward
AE9F	CAGACTCACAGTATGCATTAGG	4039	4060	Forward
AE10F	TAAARYTAGCAGGAAGATGGCCAGT	4534	4558	Forward
AE11F	CGGGTTTATTACAGGGACAGC	4899	4919	Forward
AE12F	TCAGAAGTACAYATCCCCTAGGA	5197	5220	Forward
AE13F	TTAACAGAAGATAGATGGAACAAGC	5545	5569	Forward
AE14F	CTTAGGCATCTCCTATGGCAGGAAGAAG	5956	5983	Forward
AE15F	TATTATGGGGTTCCTGTGTGG	6339	6359	Forward
AE16F	ATGGGATCAAAGTCTAAAGCCATGTG	6557	6582	Forward
AE17F	ACACATGGAATTAAGCCAGT	6966	6985	Forward
AE18F	TTTAATTGTGGAGGGGAATTTTTCT	7350	7374	Forward
AE19F	CCAGGGCAAAGAGAAGAGTGGTG	7720	7742	Forward
AE20F	GTCTGGTATAGTGCAACAGCA	7859	7879	Forward
AE21bF	CWGTGCTTTCTATAGTRAATAGAGTTAGG	8323	8351	Forward
AE22F	TTCAGCTACCACCGCTTGAGAGACT	8520	8544	Forward
AE23F	GGAGAGCCATTCTCCACATAC	8734	8754	Forward
AE24F	AAGGCTTCTTCCCTGATTGGC	9149	9169	Forward
AE1R	GCAGCTGCTTATATGCAGGATCTGAGGG	9497	9524	Reverse
AE2bR	GGTGTAACAGGCAGTTGTTYTC	9274	9295	Reverse
AE3bR	GYCTGACTGGAAAGCCTAC	8992	9010	Reverse
AE4R	GGTGAGTATCCCTGCCTAAC	8346	8365	Reverse
AE5R	AGTGCTTCCCTGCTGCTCC	7794	7811	Reverse
AE6R	TTTCTCCTCCAGGTCTGAAG	7625	7645	Reverse
AE7R	AGAAAAATTCCCCTCTACAATTA	7351	7374	Reverse
AE8R	TCCTTCTGCTAGACTGCCATTTA	7006	7028	Reverse
AE9R	GTGGGTTGGGGTCTGTGGGTACAC	6445	6468	Reverse
AE10R	CATTGCCACTGTCTTCTGCTC	6207	6227	Reverse
AE11R	CTTCTTCCCTGCCATRGGARATGCC	5960	5983	Reverse
AE12R	TTCCCGRTGKTTCCAGGGCTCTA	5853	5876	Reverse
AE13R	AATCATCACCTGCCATCTGTTTTCC	5043	5067	Reverse
AE14R	CTGTAATAAACCCGAAAATT	4893	4912	Reverse
AE15R	GAATGAATACTGCCATTTGTAAGTGC	4752	4776	Reverse
AE16R	TCACTAGCCATTGTTCTCCA	4284	4303	Reverse
AE17R	CCCATCTACATAGAAAGTCTCTGCT	3857	3881	Reverse
AE18R	TTCTGTATGTCATTGACAGTCCAGCT	3300	3325	Reverse
AE19R	CTAGGTATGGTGAATGCAGTATA	2928	2950	Reverse
AE20bR	CKTCCAATTATGTTGACAGGTGTAGGTCC	2484	2512	Reverse
AE21R	GGTGGGGCTGTTGGCTCTG	2147	2165	Reverse
AE22R	CATGCTGTCATCATTCTTCTA	1817	1838	Reverse
AE23R	CATTCTGCAGCTTCCCTCATTGAT	1402	1424	Reverse
AE24R	CTAAAGCTTCCCTTGGTGTCT	1074	1093	Reverse

Supplementary Note S1. Specificities of a randomized vaccine efficacy trial.

A randomized trial allows comparison of sequences between the two randomized groups. The design of the trial guarantees equal distribution of HIV-1 exposure in the two treatment groups. Thus, any observed difference (beyond that from sampling variability) in the distribution of viruses infecting the two groups can be attributed to the treatment assignment to vaccine. In contrast with comparative analyses of HIV-1 sequences obtained from observational studies, there is no need to take the phylogeny into account for sequence analysis in a randomized trial.

The RV144 trial was a well-conducted, double-blind randomized controlled trial. The randomization process was implemented effectively with no evidence of problems, with a high rate of effective blinding of participants during the trial, as described by Gilbert and colleagues (ref. 15). Specifically, biannual behavioral questionnaires asked trial participants about their opinion on whether they had received the candidate vaccine, the placebo or whether they did not know. At the last visit, 13,495 participants answered 'don't know' and 1301 (7.9%) provided a treatment choice, with 495 (78.8%) of 628 vaccine recipients guessing correctly and 179 (26.6%) of 673 placebo recipients guessing correctly. Based on this, we estimated that 1.8% of RV144 participants correctly perceived their treatment assignment. The estimated correct treatment perception rates were similarly low at other visits, supporting a high rate of blinding.

The statistical methods for sieve analysis made the 'no-interference' assumption that is ubiquitous in survival analysis, which for our setting states that each subject's risk of HIV-1 infection does not depend on the treatment assignment of other individuals in the study. In HIV vaccine efficacy trials, this assumption can be violated if trial participants expose one another with HIV-1. The overall rate of HIV-1 infection in the trial was 0.3% implying that inter-trial participant HIV-1 exposure was rare, although two HIV-1 transmission events were detected in the cohort (both of which had been epidemiologically documented prior to us obtaining phylogenetic evidence). Therefore, while the no-interference assumption was probably slightly violated due to two intra-study HIV-1 exposures, the amount of violation was small enough that the assessment of genotype-specific vaccine efficacy was approximately valid, providing approximately unbiased estimates of genotype-specific vaccine efficacy and correct confidence intervals and p-values.

To guard against the possibility of corruption, two phylogenetic criteria were accounted for in our dataset: HIV-1 subtypes and the presence of linked pairs.

Exclusion of non-AE sequences. Our approach consisted in excluding the sequences from the 11 subjects infected with non-CRF01_AE viruses (six in the vaccine group and five in the placebo group) to focus on if and how vaccine efficacy (VE) varies with genetic characteristics of the predominant circulating subtype. VE vs CRF01_AE viruses was estimated at 33.5% (95% CI: 7.8%-54.7%, p-value=0.034, whereas the VE vs non-CRF01_AE viruses was not significant (12.9%, 95% CI -140% to 68.4%, p-value=0.79). Thus, restricting to CRF01_AE could increase statistical power in the sieve analysis.

Linked transmission pairs. When considering the subset of CRF01_AE viruses, phylogenetic analyses showed one transmission event (between two vaccine recipients). To determine if the presence of almost identical viruses in two subjects invalidates our findings, we conducted sensitivity analyses in which we censored the data from the individual who was the second to become HIV-1 infected (AA100).